



ELSEVIER

Contents lists available at ScienceDirect

Materials Letters

journal homepage: www.elsevier.com/locate/matlet

Highly flexible, conductive and transparent PEDOT:PSS/Au/PEDOT:PSS multilayer electrode for optoelectronic devices



Mariya Aleksandrova^{a,*}, Valentin Videkov^a, Radost Ivanova^a, Ajaya K. Singh^b,
Gautam Sheel Thool^c

^a Department of Microelectronics, Technical University of Sofia, "Kl. Ohridski", Blvd., 8, 1000, Bulgaria

^b Department of Chemistry, Govt. V. Y. T. P. G. Autonomous College, Durg 491001, India

^c Inorganic and Physical Chemistry Division, CSIR-Indian Institute of Chemical Technology, Uppal Road, Tarnaka, Hyderabad 500007, India

ARTICLE INFO

Article history:

Received 4 March 2016

Received in revised form

19 March 2016

Accepted 23 March 2016

Available online 24 March 2016

Keywords:

Flexible substrate

ITO-free transparent electrode

PEDOT:PSS films

PEDOT:PSS/Au/PEDOT:PSS electrode

optoelectronic devices

ABSTRACT

The electrical, optical and bending characteristics of poly(3,4-ethylenedioxythiophene) polystyrene sulfonate (PEDOT:PSS)/Au/PEDOT:PSS deposited on polyethylene terephthalate (PET) substrate were studied as a function of inserted Au film thickness. The results were compared with those of indium-tin-oxide (ITO) and single layer PEDOT:PSS electrodes. It was found that insertion of Au film with optimized thickness between PEDOT:PSS layers improved the sheet resistance in comparison to single PEDOT:PSS film and ITO film. It was demonstrated that PEDOT:PSS(35 nm)/Au(15 nm)//PEDOT:PSS(35 nm) exhibits sheet resistance of 20.9 Ω /sq and maximum optical transmission of 82.6% in the visible region. Moreover, this multilayer electrode showed dramatically improved mechanical stability compared to ITO, when subjected to multiple bends. Its sheet resistance variation was 3.8% after applying 2000 bending cycles at radius of curvature 6 mm in comparison to 6.7% for single PEDOT:PSS film and 11.4% for ITO.

© 2016 Elsevier B.V. All rights reserved.

1. Introduction

Transparent conductive films are of great interest for application as electrodes in the variety of electronic devices, such as flat panel displays, solar cells, ion-selective membrane sensors [1–7]. They require sheet resistance 15–30 Ω /sq and transparency over 80% in the visible region. Indium-tin-oxide (ITO) is one of the most suitable materials for this purpose [8], however, the limited ductility and reliability of the ITO films when subjected to bending, restrict their application for devices fabricated on flexible substrates. Dielectric/metal/dielectric (D/M/D) structures with thin metallic film, sandwiched between transparent oxides have been extensively studied as alternative to ITO electrode [9]. Some of the most studied electrodes in this regard are $\text{Al}_2\text{O}_3/\text{Ag}/\text{Al}_2\text{O}_3$ [10], $\text{MoO}_3/\text{Ag}/\text{MoO}_3$ [11], Mn-doped tin oxide/Ag/Mn-doped tin oxide [12], $\text{ZnO}/\text{Ag}/\text{ZnO}$ [13]. Satisfying results have been achieved for optimal thicknesses of thermally evaporated Ag films in the range of 10–18.8 nm and 40–70 nm sputtered metal-oxide films. Sheet resistance in the range of 13–4.98 Ω /sq, transparency in the visible region 84–88%, and great stability of the sheet resistance, with negligible variation at bending up to 1000 cycles have been obtained for the different multilayer structures. The low value of the

sheet resistance is usually ascribed to the presence of Ag film with optimized thickness.

Due to the expensive deposition methods (such as magnetron sputtering and its modifications) and the required precise setting of the deposition conditions, the most recent studies have been focused on replacement of the metal-oxide films by conductive polymers. In contrast to the metal-oxides, the polymers are characterized by higher elasticity and possibility for low cost "wet" deposition methods. In this regard, one of the most promising materials is PEDOT:PSS, which is also used as conductive material for touch screens and flexible organic solar cell [14,15]. It is typically deposited by ink-jet printing, spin-coating, or electrophoresis [16,17]. PEDOT:PSS films show transparency beyond 80% in the visible region, but exhibits much higher resistivity (~ 70 – 300Ω /sq) than ITO and the other D/M/D systems. To overcome this problem, different approaches have been applied, such as Ag nanoparticles forming grid with different meshes in combination with PEDOT:PSS and ZnO [18], gold-nanoparticle-doped single-walled carbon nanotubes [19], graphene/multiwalled carbon nanotube [20], organic/metal/organic (O/M/O) structures, containing few types of conductive polymers with different thicknesses [21]. The results have been promising in point of mechanical stability, namely less than 2% variation of the resistivity after 300 bends at 9.5 mm radius of curvature at up to 13 Ω /sq and transparency $\sim 85\%$. However, the reported structures are rather complex and involve expensive materials and/or deposition techniques.

* Corresponding author.

E-mail address: m_aleksandrova@tu-sofia.bg (M. Aleksandrova).

In this study simple cost-effective multilayer electrode PEDOT:PSS/Au/PEDOT:PSS is fabricated on PET substrate. Au films are more ductile, compared to the silver ones and the mechanical stability of the electrode is assumed to be superior over the existing solutions. The electrical and optical properties of the PEDOT:PSS/Au/PEDOT:PSS are studied as a function of the Au film thickness and the number of supplied bending cycles. The suggested structures exhibit significantly improved electrical properties, as compared to single layer PEDOT:PSS. Moreover, the characteristics measured are comparable to those of ITO films and to the latest reported results for D/M/D and O/M/O electrodes, and even exceed them in mechanical durability. This indicates the great potential of the suggested multilayer structures for application as transparent electrode in flexible optoelectronic devices.

2. Materials and methods

PEDOT:PSS/Au/PEDOT:PSS samples were deposited on ultrasonically cleaned PET substrates. The PET pieces were exposed to ultraviolet (UV) light (365 nm, 250 W) in advance per 5 min to improve the wetting conditions and adhesion of the bottom PEDOT:PSS films [22]. PEDOT:PSS solution (1.1% in H₂O, Sigma Aldrich) was spin-coated on the UV treated PET at 2000 rpm per 50 sec and dried at 70 °C per 10 min for achieving 35 nm thin films. Subsequently, different samples were prepared, consisting low temperature DC sputtered Au films with thicknesses of 10, 15, 20 and 25 nm. Finally, on the Au coatings, top PEDOT:PSS films were spin-coated with the same thickness. For comparison, ITO film (In₂O₃:SnO₂=95:5 mol%) was RF sputtered on PET at power of 60 W, under oxygen partial pressure of 2.10⁻⁴ Torr and total working pressure of 2.5.10⁻² Torr. In addition, single spin-coated PEDOT:PSS films were also provided.

Four point probe setup (FPP5000) was used for the sheet and specific resistance measurements. Transmittance of the samples was recorded with a UV-vis Specord spectrograph. X-ray photoelectron spectroscopy (XPS) was conducted on the top PEDOT:PSS films, using ESCALAB Mk II spectrometer with aluminum radiation ($h\nu = 1486.6$ eV). Films thicknesses were measured by ellipsometry. The mechanical durability of the samples was tested by a home made bending setup with movable holder, vibrating at certain frequency and facing plate regulated for obtaining different radii of curvature. In this case cyclic inner/outer bending of the flexible substrates at radius of 6 mm was set. For intermediate monitoring of the cracks revealed in the samples, optical microscopy at magnification of 500 was used after certain set of cycles.

3. Results and discussion

The sheet resistance measured for PEDOT:PSS(35 nm)/Au/PEDOT:PSS(35 nm) sharply decreased from 150 to 20.9 Ω/sq as the Au thickness increased from 10 nm to 15 nm, afterward the decrease was slighter. The specific resistance followed the same trend (i.e. decreased from 0.412 Ω cm to 0.117 Ω cm, respectively). For the PEDOT:PSS and ITO films each with thickness of 35 nm, sheet resistances of 49.9 Ω/sq and 47.3 Ω/sq were measured. The results are summarized in Table 1. Fig. 1a shows the resistivity (ρ) and sheet resistance (R_s) of PEDOT:PSS(35 nm)/Au/PEDOT:PSS (35 nm) multilayer electrode as a function of the Au thickness. It is known that the morphology of vacuum deposited metal films is depended on the thickness. Usually, 10 nm thin metal films (and particularly Au films) consist of disjoined particles and randomly

distributed islands [23,24]. Thicker than 10 nm metal films, including Au, form continuous coating and denser surface [10,25,26]. This may be the possible reason for the highest value of R_s achieved for electrode with 10 nm Au film and for the lowest value at 25 nm Au film, respectively. The irregular 10 nm Au film probably leads to formation of inhomogeneous top PEDOT:PSS film, resulting in non-uniform contact with the FPP probes, causing in this way high measured resistance. Although the best results for the conductivity were achieved at Au 25 nm, the sample with 15 nm thick Au film was selected as optimal for further study, due to its better transparency in the visible region.

Enhancement in the carriers' concentration by a factor of 1.6–3 and increase in charge carrier mobility can be noticed from Table 1 for the structures with Au film thickness between 15 and 25 nm. One of the PEDOT:PSS functions in organic optoelectronic devices is hole transport, because of its suitable band alignment with respect to the other components in the structure. Therefore, the enhancement of PEDOT:PSS/Au/PEDOT:PSS conductivity is desired effect for reducing the turn-on voltage and the contact resistance. The increase in the conductivity is result from the increase of carriers' concentration and mobility, which suggested Ohmic injecting contact at the Au/top PEDOT:PSS interface. This approach might be used for energy level alignment at the interfaces without chemical doping of the PEDOT:PSS films. In order to evaluate the flexibility of the prepared multilayer structures onto PET substrates, samples were tested at repeating outer/inner bends. PEDOT:PSS/Au(15 nm)/PEDOT:PSS sample exhibited sheet resistance variation of 3.8% after 2 000 bends and the PEDOT:PSS/Au(20 nm)/PEDOT:PSS sample – 3.6% variation at the same number of bends. For comparison, the variation of the sheet resistance for PEDOT:PSS and ITO films on PET at the same conditions was 6.7% and 11.4%, respectively. As expected, the sheet resistance of ITO film sharply increased to 6.3% even at 200 cycles, due to the cracks formed in the film. On the other hand, during the bending test, the sheet resistance for both PEDOT:PSS/Au/PEDOT:PSS multilayer electrodes remained almost unchanged even after 2000 bends. This electro-mechanical stability is due to the presence of ductile Au film with high failure strain. Moreover, it is known that the spin coated PEDOT:PSS films have amorphous structure with failure strain higher than that of crystalline films [27,28]. Conductivity degradation for all polymeric based samples occurred at ~ 20,000 cycles. The variation of R_s at this ultimate value was as follow: for PEDOT:PSS film – 8.4%; for PEDOT:PSS/Au(15 nm)/PEDOT:PSS – 5.7%; for PEDOT:PSS/Au(20 nm)/PEDOT:PSS – 5.9%, for ITO film – 13.5%. Fig. 1b shows the relative change in the sheet resistance of PEDOT:PSS/Au(15 nm)/PEDOT:PSS multilayer electrode on PET, as a function of the number of bending cycles. This change was defined as $\Delta R/R_s = R_s - R_{s0}/R_{s0}$, where R_{s0} is the initial resistance and R_s is the measured resistance after bending.

To exclude possible diffusion of Au particles in the PEDOT:PSS layer, XPS analysis of the top polymer coating of the PEDOT:PSS/Au/PEDOT:PSS samples were conducted. The peak of core level C 1s spectrum is shown in Fig. 2a. Two components with binding energies at 285.8 eV and 288.7 eV are revealed, corresponding to

Table 1

Resistivity, sheet resistance, charge carriers concentration and mobility, obtained for PEDOT:PSS(35 nm)/Au(10,15,20,25 nm)/PEDOT:PSS(35 nm) multilayer electrode, single layer PEDOT:PSS and ITO film, deposited on PET substrate.

Sample	Sheet resistance (R_s), Ω/sq	Resistivity (ρ), Ω cm	Carriers concentration, cm ⁻³	Carriers mobility, cm ² /V s
PEDOT:PSS (35 nm)/ Au (10 nm)/PEDOT:PSS (35 nm)	~ 150	0.412	2.1×10^{14}	0.0125
PEDOT:PSS (35 nm)/ Au (15 nm)/PEDOT:PSS (35 nm)	20.9	0.153	3.4×10^{14}	0.0136
PEDOT:PSS (35 nm)/ Au (20 nm)/PEDOT:PSS (35 nm)	9.05	0.123	5.2×10^{14}	0.0149
PEDOT:PSS (35 nm)/ Au (25 nm)/PEDOT:PSS (35 nm)	6.47	0.117	7.4×10^{14}	0.0205
PEDOT:PSS (35 nm)	49.9	0.21	0.8×10^{14}	0.0081
ITO (35 nm)	47.3	0.131	10^{20}	31

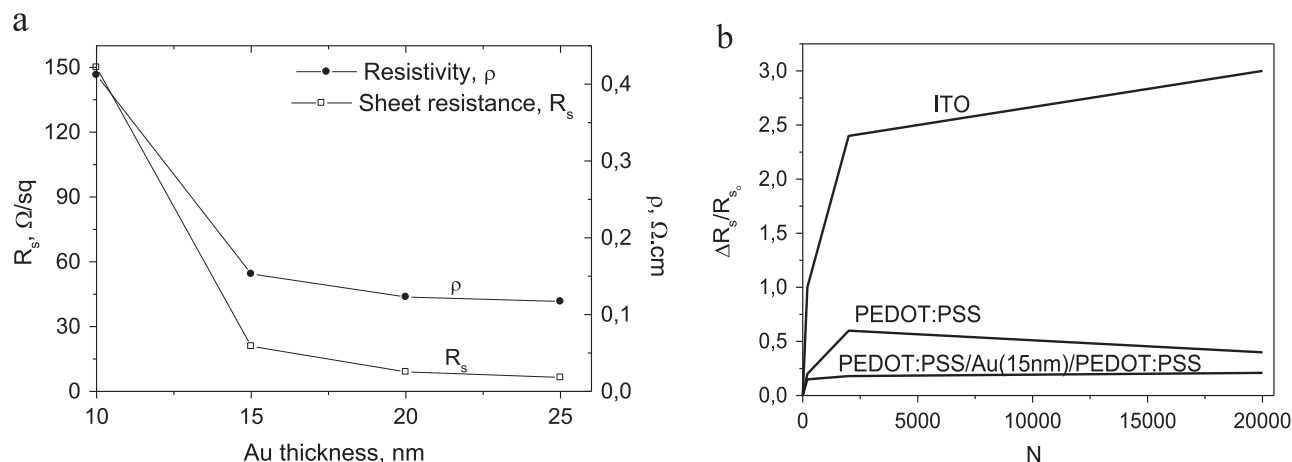


Fig. 1. (a) Sheet and specific resistance of PEDOT:PSS/Au/PEDOT:PSS electrodes as a function of the Au thickness; (b) relative change in the sheet resistance of multilayer electrode PEDOT:PSS/Au (15 nm)/PEDOT:PSS, PEDOT:PSS and ITO films on PET substrate, as a function of the number of bending cycles.

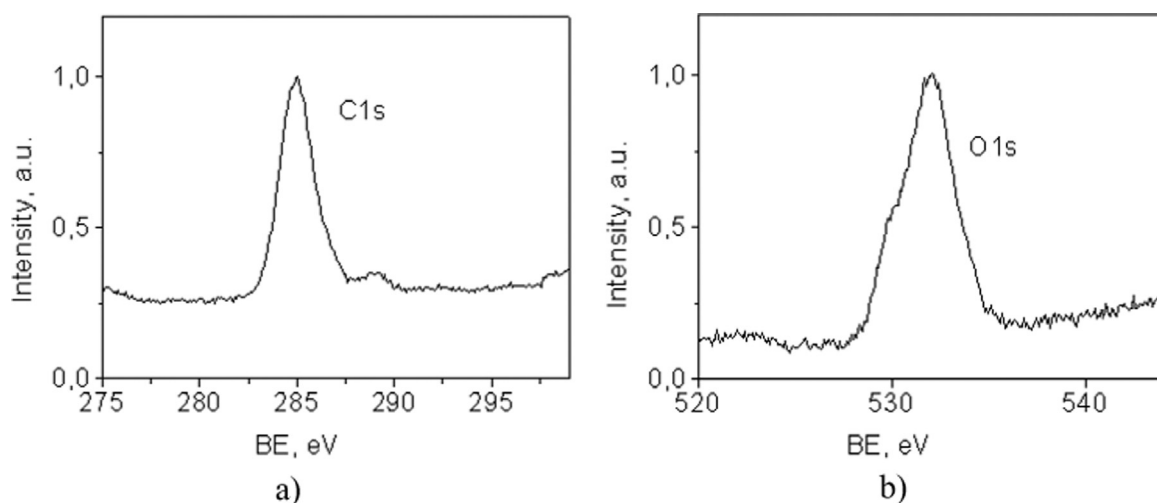


Fig. 2. XPS of PEDOT:PSS top film from the PEDOT:PSS/Au/PEDOT:PSS system.

(C-C-O) and (C-S) bonds of the PEDOT and PSS, respectively [29].

XPS spectrum for the O 1s peak is shown in Fig. 2b. It reveals major component with binding energy at 533.1 eV, assigned to the (C-O-C) of the PEDOT [30]. The results obtained did not suggest modification of the electron charge distribution along the C-O-C backbone of the PEDOT:PSS, caused by dissolution of Au. Presence of Au particles in the polymer film would shift vastly the characteristic peaks of C 1s and O 1s to lower binding energies. Therefore, the mechanisms responsible for the enhanced conduction can be explained with sharp and Ohmic Au/top PEDOT:PSS interface without mixture of both components. Further studies by ultraviolet photoelectron spectroscopy and transmission electronic microscopy are necessary to examine the energy levels alignment and the coatings interfaces.

Fig. 3 shows the transparency in the visible region of the multilayer electrode PEDOT:PSS/Au/PEDOT:PSS with different thicknesses of the Au film (15 nm and 20 nm). Both spectra follow similar trend – gradually increase, reaching maximum at 485 nm for Au 20 nm and in the range of 485–525 nm for Au 15 nm, and then slightly decrease with increase in the wavelength. Maximum transmittance is measured to be 82.6% and 81.5% for electrode with Au 15 nm and 20 nm, respectively. The plateau of the transmission maximum became narrower and less transparent when Au thickness increases. In our previous study it was shown that the single layer PEDOT:PSS and ITO films exhibited maximum transmittance $\sim 80\%$ and 80.5% at 470 nm [22]. The improvement

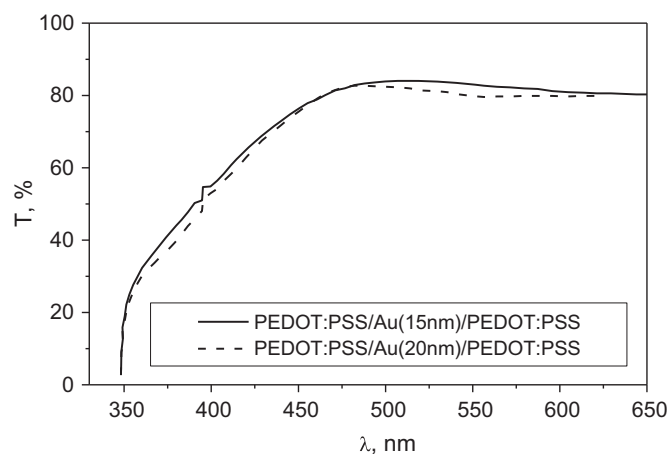


Fig. 3. Transmittance in the visible region, measured for PEDOT:PSS/Au/PEDOT:PSS samples on PET with different thickness of the Au film.

in the maximum transparency for this multilayer system can be ascribed to plasmon coupling effect, due to the large difference between the refractive indices of the materials used [31]. The optical transmittance window at wavelengths around 550 nm is wider for PEDOT:PSS/Au/PEDOT:PSS as compared to ITO, which might be ascribed to plasmon-absorption-dependent reflections

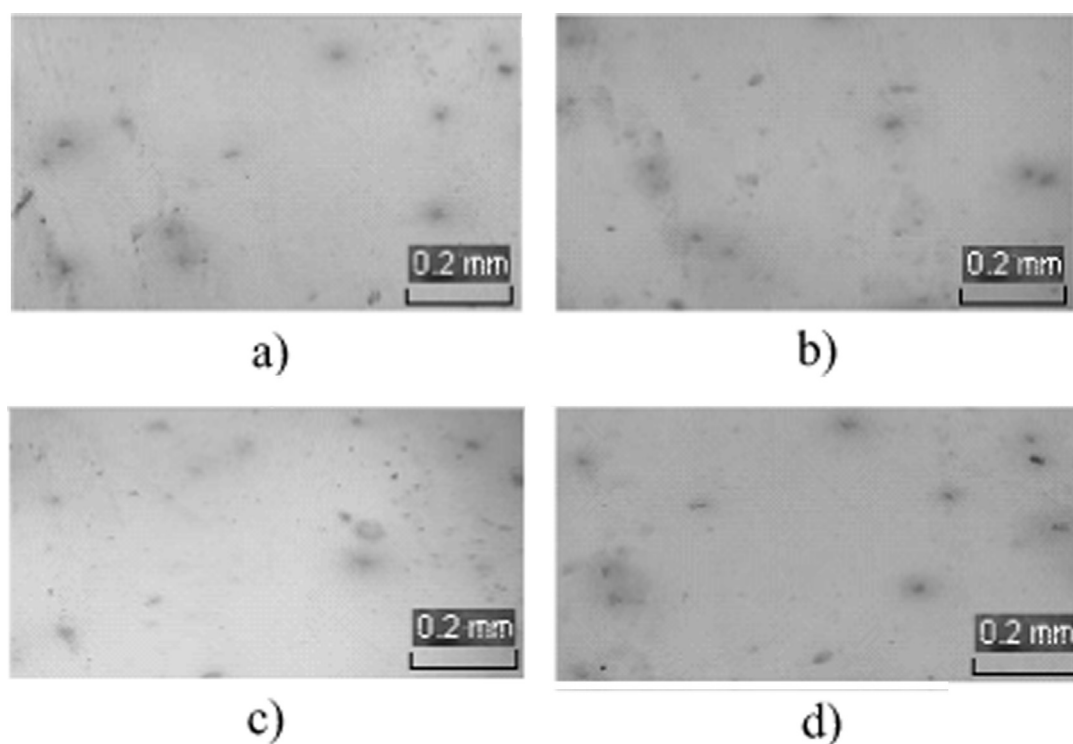


Fig. 4. Optical micrographs of the samples surfaces: (a) and (b) correspond to PEDOT:PSS/Au(15 nm)/PEDOT:PSS before and after 2000 bends; (c) and (d) correspond to PEDOT:PSS/Au(20 nm)/PEDOT:PSS before and after 2000 bends.

[13,32]. Although, samples with 10 nm and 25 nm Au films were also prepared, their UV–vis spectra are not shown, due to unsatisfied results - the sample with Au 10 nm showed high transparency, but also too high, unsuitable for electrode purposes sheet resistance of hundreds Ω/sq . The sample with Au 25 nm showed less than 74% transparency.

Optical microscopy images (Fig. 4a–d) confirmed lack of cracks in the multilayer electrodes at bends up to 2 000, which is in agreement with the results for $\Delta R/R_{s_0}$.

4. Conclusion

In summary, we have shown that the optical, electrical and mechanical properties of PEDOT:PSS/Au/PEDOT:PSS multilayer electrode deposited on flexible substrate are function of the golden film thickness. The Au film with thickness 15 nm was found to be the most suitable as front panel electrode in the optoelectronic devices, because of its low sheet resistance (20.9 Ω/sq) and high transparency in the visible region (82.6%). Moreover, this sample also showed high electrical and mechanical stability after applying of great number bending cycles – 3.8% resistance variation after 2 000 bends. The results revealed the great potential for application of the PEDOT:PSS/Au/PEDOT:PSS multilayer system as highly transparent, conductive and flexible electrode in optoelectronic devices.

Acknowledgments

The work is financial supported by grants DMU 03/5–2011 of Fund “Scientific Research”, Bulgarian Ministry of Education and Science (equipment and Au provided) and 141PR0005-03 funded by Scientific and Research Sector of Technical University of Sofia (PEDOT:PSS provided).

References

- [1] S. Sohn, Y.S. Han, Transparent conductive oxide (TCO) films for organic light emissive devices (OLEDs), organic light emitting diode - material process devices, InTech (2011).
- [2] X.G. Li, H. Feng, M.R. Huang, G.L. Gu, M.G. Moloney, Ultrasensitive Pb(II) potentiometric sensor based on copolyaniline nanoparticles in a plasticizer-free membrane with a long lifetime, *Anal. Chem.* 84 (2012) 134–140.
- [3] M.R. Huang, Y.B. Ding, X.G. Li, Y.J. Liu, K. Xi, C.L. Gao, R.V. Kumar, Synthesis of semiconducting polymer microparticles as solid ionophore with abundant complexing sites for long-life Pb(II) sensors, *ACS Appl. Mater. Interfaces* 6 (2014) 22096–22107.
- [4] M.R. Huang, Y.B. Ding, X.G. Li, Lead-ion potentiometric sensor based on electrically conducting microparticles of sulfonic phenylenediamine copolymer, *Analyst* 138 (2013) 3820–3829.
- [5] M.R. Huang, Y.B. Ding, X.G. Li, Combinatorial screening of potentiometric Pb (II) sensors from polysulfamoanthraquinone solid ionophore, *ACS Comb. Sci.* 16 (2014) 128–138.
- [6] M.R. Huang, X.W. Rao, X.G. Li, Y.B. Ding, Lead ion-selective electrodes based on polyphenylenediamine as unique solid ionophores, *Talanta* 85 (2011) 1575–1584.
- [7] X.-G. Li, X.-L. Ma, M.R. Huang, Lead(II) ion-selective electrode based on polyaminoanthraquinone particles with intrinsic conductivity, *Talanta* 78 (2009) 498–505.
- [8] H. Hosono, H. Ohta, M. Orita, K. Ueda, M. Hirano, Frontier of transparent conductive oxide thin films, *Vacuum* 66 (2002) 419–425.
- [9] I.P. López, L. Cattin, D.T. Nguyen, M. Morsli, J.C. Bernède, Dielectric/metal/dielectric structures using copper as metal and MoO_3 as dielectric for use as transparent electrode, *Thin Solid Films* 520 (2012) 6419–6423.
- [10] J.A. Jeong, H.K. Kim, $\text{Al}_2\text{O}_3/\text{Ag}/\text{Al}_2\text{O}_3$ multilayer thin film passivation prepared by plasma damage-free linear facing target sputtering for organic light emitting diodes, *Thin Solid Films* 547 (2013) 63–67.
- [11] T. Abachi, L. Cattin, G. Louarn, Y. Lare, A. Bou, M. Makha, P. Torchio, M. Fleury, M. Morsli, M. Addou, J.C. Bernède, Highly flexible, conductive and transparent $\text{MoO}_3/\text{Ag}/\text{MoO}_3$ multilayer electrode for organic photovoltaic cells, *Thin Solid Films* 545 (2013) 438–444.
- [12] C.H. Lee, R. Pandey, B.Y. Wang, W.K. Choi, D.K. Choi, Y.J. Oh, Nano-sized indium-free MTO/Ag/MTO transparent conducting electrode prepared by RF sputtering at room temperature for organic photovoltaic cells, *Sol. Energy Mater. Sol. Cells* 132 (2015) 80–85.
- [13] J.H. Kim, J.H. Lee, S.W. Kim, Y.Z. Yoo, T.Y. Seong, Highly flexible ZnO/Ag/ZnO conducting electrode for organic photonic devices, *Ceram. Int.* 41 (2015) 7146–7150.
- [14] H. Yan, T. Jo, H. Okuzaki, Potential application of highly conductive and transparent poly(3,4-ethylenedioxythiophene)/poly(4-styrenesulfonate) thin films to touch screen as a replacement for indium tin oxide electrode, *Polym. J.*

- 43 (2012) 662–665.
- [15] J.G. Tait, B.J. Worfolk, S.A. Maloney, T.C. Hauger, A.L. Elias, J.M. Buriak, K. D. Harris, Spray coated high-conductivity PEDOT:PSS transparent electrodes for stretchable and mechanically-robust organic solar cells, *Sol. Energy Mater. Sol. Cells* 110 (2013) 98–106.
- [16] A. Singh, S. Mandal, V. Singh, A. Garg, M. Katiyar, Inkjet printed PEDOT:PSS for organic devices, in: *Proceedings of the SPIE vol. 8549, 16th International Workshop on Physics of Semiconductor Devices*, 15 October 2012, Kanpur, India.
- [17] B.J. Kim, S.H. Han, J.S. Park, Properties of CNTs coated by PEDOT:PSS films via spin-coating and electrophoretic deposition methods for flexible transparent electrodes, *Surf. Coat. Tech.* 271 (2015) 22–26.
- [18] I. Kim, S.W. Kwak, Y. Ju, G. Park, T. Lee, Y. Jang, Y. Choi, D. Kang, Roll-offset printed transparent conducting electrode for organic solar cells, *Thin Solid Films* 580 (2015) 21–28.
- [19] N.R. Shin, S.H. Choi, J.Y. Kim, Highly conductive PEDOT:PSS electrode films hybridized with gold-nanoparticle-doped-carbon nanotubes, *Synth. Met* 192 (2014) 23–28.
- [20] S. Yadav, V. Kumar, S. Arora, S. Singh, D. Bhatnagar, I. Kaur, Fabrication of ultrathin, free-standing, transparent and conductive graphene/multiwalled carbon nanotube film with superior optoelectronic properties, *Thin Solid Films* 595 (2015) 193–199.
- [21] X. Guo, X. Liu, F. Lin, H. Li, Y. Fan, N. Zhang, Highly conductive transparent organic electrodes with multilayer structures for rigid and flexible optoelectronics, *Sci. Rep.* 5 (2015) 10569.
- [22] M. Aleksandrova, N. Kurtev, V. Videkov, S. Tzanova, S. Schintke, Material alternative to ITO for transparent conductive electrode in flexible display and photovoltaic devices, *Microelectron. Eng.* 145 (2015) 112–116.
- [23] G.D. Sockalingum, A. Beljebbar, H. Morjani, J.F. Angiboust, M. Manfait, Characterization of island films as surface-enhanced Raman spectroscopy substrates for detecting low antitumor drug concentrations at single cell level, *Biospectroscopy* 4 (1998) S71–S78.
- [24] K. Uozumi, Observation of very thin gold island films vacuum-deposited onto MoS₂ surface by STM, *J. Microsc.* 152 (1988) 193–196.
- [25] J.A. Jeong, H.K. Kim, Low resistance and highly transparent ITO–Ag–ITO multilayer electrode using surface plasmon resonance of Ag layer for bulk-heterojunction organic solar cells, *Sol. Energy Mater. Sol. Cells* 93 (2009) 1801–1809.
- [26] L. Cattin, S. Tougaard, N. Stephant, S. Morsli, J.C. Bernède, On the ultrathin gold film used as buffer layer at the transparent conductive anode/organic electron donor interface, *Gold. Bull.* 44 (2011) 199–205.
- [27] N. Massonnet, A. Carella, A. de Geyer, J.F. Vincent, J.P. Simonato, Metallic behaviour of acid doped highly conductive polymers, *Chem. Sci.* 6 (2015) 412–417.
- [28] H. Jeong, J. Kim, T. Yoon, S. Choi, Bipolar resistive switching characteristics of poly(3,4-ethylene-dioxythiophene): poly(styrenesulfonate) thin film, *Curr. Appl. Phys.* 10 (2010) 46–49.
- [29] A.A. Farah, S.A. Rutledge, A. Schaarschmidt, R. Lai, J.P. Freedman, Conductivity enhancement of poly(3,4-ethylenedioxythiophene)-poly(styrenesulfonate) films post-spincasting, *J. Appl. Phys.* 112 (2012) 113709.
- [30] D. Briggs, G. Beamson, XPS studies of the oxygen 1s and 2s levels in a wide range of functional polymers, *Anal. Chem.* 65 (1993) 1517–1523.
- [31] T.G. Chen, B.Y. Huang, E.C. Chen, P. Yu, H.F. Meng, Micro-textured conductive polymer/silicon heterojunction photovoltaic devices with high efficiency, *Appl. Phys. Lett.* 101 (2012) 033301.
- [32] S. Yu, W. Zhang, L. Li, D. Xu, H. Dong, Y. Jin, Optimization of SnO₂/Ag/SnO₂ trilayer films as transparent composite electrode with high figure of merit, *Thin Solid Films* 552 (2014) 150–154.